

Key Points:

- Intense tropical cyclone genesis frequency in southeastern western North Pacific shows an asymmetric response to the Victoria mode (VM), rising during positive VM phases
- The asymmetric response is driven by differing impacts of positive and negative VM phases on environmental factors like sea surface temperature and wind shear

Correspondence to:

Q. Zhong and R. Ding,
zqj@lasg.iap.ac.cn;
drq@bnu.edu.cn

Citation:

Wen, T., Li, J., Tu, S., Zhong, Q., Ding, R., & Ming, Z. (2025). Asymmetric influence of the North Pacific Victoria mode on intense tropical cyclone formation in the western North Pacific. *Journal of Geophysical Research: Oceans*, 130, e2025JC022505. <https://doi.org/10.1029/2025JC022505>

Received 14 FEB 2025

Accepted 7 AUG 2025

Author Contributions:

Conceptualization: Tao Wen, Quanjia Zhong
Formal analysis: Tao Wen
Funding acquisition: Quanjia Zhong, Ruiqiang Ding
Investigation: Zhang Ming
Methodology: Tao Wen
Resources: Ruiqiang Ding
Software: Zhang Ming
Supervision: Ruiqiang Ding
Validation: Zhang Ming
Visualization: Tao Wen
Writing – original draft: Tao Wen
Writing – review & editing: Jianping Li, Shifei Tu, Quanjia Zhong, Ruiqiang Ding

Asymmetric Influence of the North Pacific Victoria Mode on Intense Tropical Cyclone Formation in the Western North Pacific

Tao Wen^{1,2}, Jianping Li^{3,4} , Shifei Tu⁵ , Quanjia Zhong⁶ , Ruiqiang Ding^{1,7} , and Zhang Ming^{1,7}

¹State Key Laboratory of Earth Surface Processes and Hazards Risk Governance (ESPHR), Beijing Normal University, Beijing, China, ²School of Resources and Environmental Science, Quanzhou Normal University, Quanzhou, China, ³Frontiers Science Center for Deep Ocean Multi-spheres and Earth System (DOMES)/Key Laboratory of Physical Oceanography/Academy of Future Ocean/College of Oceanic and Atmospheric Sciences/Center for Ocean Carbon Neutrality, Ocean University of China, Qingdao, China, ⁴Laboratory for Ocean Dynamics and Climate, Qingdao Marine Science and Technology Center, Qingdao, China, ⁵South China Sea Institute of Marine Meteorology / College of Ocean and Meteorology, Guangdong Ocean University, Zhanjiang, China, ⁶Center for Ocean Research in Hong Kong and Macau, Department of Ocean Science and Department of Mathematics, The Hong Kong University of Science and Technology, Hong Kong, China, ⁷Key Laboratory of Environmental Change and Natural Disasters of Chinese Ministry of Education / Faculty of Geographical Science, Beijing Normal University, Beijing, China

Abstract This study investigates the asymmetric response of intense tropical cyclone (TC) genesis frequency (tropical cyclone genesis frequency (TCGF)) in the southeastern western North Pacific (SE-WNP) to the Victoria mode (VM) from 1950 to 2022. We show a significant increase during the positive VM phases but only a slight decrease during the negative VM phases, indicating a nonlinear relationship between intense TCGF and VM. Observational analyses and numerical simulations demonstrate that this asymmetric response is primarily associated with differing effects of positive and negative VM events on environmental conditions, which subsequently affect TC genesis and development. Specifically, during positive VM years, there is a notable positive sea surface temperature anomaly over the SE-WNP combined with enhanced relative vorticity and weakened vertical wind shear, which creates favorable conditions for intense TC genesis. This study highlights the complex relationship between extratropical climate models and TC activity and has significant implications for predicting intense TCs in the SE-WNP.

Plain Language Summary Tropical cyclones (TCs) are some of the most destructive natural hazard events worldwide, resulting in substantial loss of life and major economic impacts across the globe. TC activity of western North Pacific (WNP) is influenced by a range of climate modes, with the Victoria mode (VM) being one of the most important extratropical forcings. This study reveals an asymmetric response of intense TC genesis frequency (TCGF) in the southeastern part of the WNP to the VM. Specifically, the frequency and proportion of intense TCs exhibit a significant increase during the positive VM phase but only a slight decrease during the negative VM phase, indicating a nonlinear TCGF-VM relationship. Observational analyses and numerical simulations demonstrate that this asymmetric response arises from the varying influences of the positive and negative VM events on atmospheric conditions, which subsequently affect TC genesis and development. Collectively, this work advances prognostic frameworks for high-intensity TC over SE-WNP, as well as for the enhancement of strategies for disaster prevention against the impacts of intense TCs in littoral East Asia.

1. Introduction

Tropical cyclones (TCs) are among the most devastating events to affect the world, causing significant human and economic casualties on a global scale (Huang et al., 2024; Kunze, 2021; Murnane & Elsner, 2012). As the epicenter of global cyclonic activity, the western North Pacific (WNP) hosts approximately one-third of annual occurrences (Chen et al., 2023; Guo & Tan, 2018; Zhan et al., 2022), with ~80% of category 4–5 systems—disproportionately incurring ~50% of regional disaster impacts—emerging from its southeast (SE-WNP; Huang et al., 2022; Kunze, 2021; Li et al., 2015). Thus, improving our understanding the change in the intense TC genesis frequency (TCGF) over the SE-WNP is of scientific and social importance.

Many studies suggested that the temporal variability of TC activity over the SE-WNP is modulated by various climate modes, such as Pacific decadal oscillation (PDO), El Niño–Southern Oscillation (ENSO), Pacific meridional mode (PMM; Kim et al., 2020; Li et al., 2018; Scoccimarro et al., 2021; Song et al., 2023; Wang, Li, Jin, et al., 2019; Wang & Wu, 2023; Wu & Lin, 2012), and several other factors (Wang, Li, Li, et al., 2019). Scoccimarro et al. (2021) reported that TC activity over WNP exhibits asymmetric changes under different phases of PDO. During the negative PDO phase, enhanced frequency and intensity of Central Pacific (CP) La Niña events lead to suppressed the TC generation over WNP (Kim et al., 2020). Similarly, Song et al. (2023) suggested that the variations in large-scale environmental responses to the positive/negative PMM phases result in an asymmetric TC frequency–PMM teleconnection over WNP.

As the second principal component of the extratropical Pacific sea surface temperature (SST) anomaly (SSTA) mode over the North Pacific (Salinger et al., 2001), the Victoria mode (VM) can act as a bridge between the extratropical regions of the North Pacific and the tropical ocean (Ding, Li, Tseng, & Ruan, 2015; Ding, Li, Tseng, Sun, & Guo, 2015, 2022; Ji et al., 2024). Consequently, it exerts a considerable influence on extreme weather and climatological events (e.g., TC, heavy rainfall, marine heatwaves) on the global and regional scale (Di Lorenzo & Mantua, 2016; Ding et al., 2023; Newman et al., 2016). Particularly, VM is one of the most important factors, besides PMM and ENSO (Song et al., 2023; Wang & Wu, 2023), modulating WNP TC activity, especially on annual and decadal scales (Ji et al., 2024). For instance, previous study demonstrated that the spring VM affects the subsequent summer's TC genesis location over WNP, showing a positive correlation with TCGF in the eastern part of the WNP but a negative correlation with TCGF in the western part of the WNP (Pu et al., 2019). This study improved our understanding of extratropical factors affecting the seesaw variability in genesis location of TCs over the whole WNP basins. However, they still do not address the influences of the VM on the TC activity in a specified subbasin, such as SE-WNP, where most of intense TCs are mainly formed. Particularly, it is still unclear whether the TC activity in this region shows an asymmetric response to VM over extended time periods. The frequency of intense TC formation not only influences preparedness and mitigation strategies but also has profound implications for global and regional climate. Therefore, analyzing and comparing the anomalies features of the SE-WNP TCGF during different VM phases are essential for enhancing disaster prevention and mitigation efforts in East Asian coastal countries.

This study follows the analytical structure outlined below: The second section describes the observational data sets and diagnostic framework. The analysis then divides into two parts—Section 3 quantifies VM phase-dependent variations in SE-WNP TCGF, while Section 4 examines concurrent changes in synoptic-scale environmental precursors. The final section summarizes the mechanisms leading to such asymmetric responses.

2. Data and Methodology

Tropical cyclone analytics leverage 1950–2022 best-track reanalysis archives (6-hourly resolution; CMA), calibrated through canonical homogeneity frameworks (Knapp et al., 2010; Lu et al., 2021). Intensity stratification follows 10-min sustained wind protocols: typhoon (TY; 32.7–41.4 m/s), strong typhoon (STY; 41.5–50.9 m/s), and super typhoon (SuTY; ≥ 51.0 m/s), per basin-operational Saffir–Simpson adaptations (Ying et al., 2014). Cyclonic activity is centered on June to October (JJASO) intraannual climatology. Meanwhile, we curated multiagency best track archives (JTWC–JMA) to ensure methodological fidelity (Knapp et al., 2010). Subsynchronous diagnostics harness NCEP/NCAR (Kalnay et al., 1996) 2.5°-resolution gridded predictors—midlevel humidity (600 hPa), low-level vorticity (850 hPa), upper divergence (200 hPa), and deep-layer vertical wind shear (VWS; 850–200 hPa).

Following in the study of Vimont et al. (2003), the VM diagnostics derived from orthogonalized temporal modes (principal components) associated with the secondary EOF mode of extratropical North Pacific SST anomalies (SSTAs; 20–65°N, 124°E–100°W) spanning 1950–2022. Based on the magnitude of the 3-month average FMA VM index, a positive (or negative) VM event is defined as a year when the FMA VM index is greater than (or equal to) one standard deviation or less than one negative standard deviation.

This study employs the CESM v1.2.2.1 coupled model (Hurrell et al., 2013) to investigate the hierarchical impacts of the VM on TC genesis environments over the WNP. The CESM is a state-of-the-art, fully coupled, global climate model developed at NCAR to simulate the whole Earth system. CESM consists of atmospheric, ocean, ice, land surface, and other components. Its atmospheric component is the Community Atmosphere Model version 5, with a horizontal resolution of about 1° (1.25° × 0.9°) and 30 layers in the vertical, and its ocean component is the Parallel Ocean Program version 2, with a similar horizontal resolution and 60 layers in the

vertical. The land and sea ice model of CESM are the Community Land Model version 4 and Los Alamos Sea Ice Model version 4 (CICE4). This experiment was conducted in two steps. First, a simulation of the preindustrial climate state over 120 years, based on radiative forcing in 1850, is carried out using a fully coupled model between the atmosphere and ocean in order to establish the climatological baseline. Second, sensitivity experiments with positive/negative VM forcing are performed, each comprising 30 ensemble members. The VM-related SST anomalies are derived from historical observations (1950–2022) via linear regression of the VM index onto monthly SST fields, with the resulting patterns normalized to $\pm 1\sigma$ intensity (equivalent to the standard deviation of observed extreme VM events). To accurately impose these anomalies in CESM, a nudging technique (relaxation timescale $\tau = 10$ days) is applied over the North Pacific (0° – 60° N, 100° E– 100° W) while allowing free SST evolution elsewhere. That is, the sensitivity experiments used a hybrid coupling of regional constraints plus free coupling. Each sensitivity experiment spans 14 months (January–February cycle) to capture seasonal linkages between VM and TC activity.

We examine the correlation between the VM index and the frequency of TC using linear correlations and compositional analysis, respectively, and then use the two-tailed Student's *t*-test to assess the robustness of the results. Given TC annual counts conform to skewness-limited Poisson processes (Chu et al., 2010; Ji et al., 2024), the statistical significance of genetic differences between periods is tested using a nonparametric bootstrap method (Li et al., 2013; Pyper & Peterman, 1998).

3. Asymmetric Response of the SE-WNP TCGF to the VM

Figure 1 illustrates a significant positive connection between the VM index during February to April (FMA) and the averaged SE-WNP TCGF during the following TC seasons for the period 1950–2022 ($R = 0.51$; significant at the 95% confidence level). Although the effect of ENSO is removed through partial correlation analysis, the relationship between FMA VM and JJASO TCGF remains significant (Figure 1a). This relationship is also observed in both the JTWC and JMA data sets, further confirming the robustness of our results (figures not shown). The scatter plot of FMA VM and JJASO TCGF presents a significant concentration of data points in the first and third quadrants (Figure 1c). Considering the uncertainty of TC data due to the absence of satellites prior to the 1970s, the SE-WNP TCGF and VM are subjected to further scrutiny across the 1980–2022 epoch (Figure 1b), with results similar to those in Figure 1. This finding indicates that the interannual variability of TCGF over the SE-WNP is closely linked to FMA VM but independent of ENSO effects.

As the SE-WNP is the intense TCs nursery (Huang et al., 2022), we further explore the relationship between SE-WNP intense TCs frequency and the FMA VM index from 1950 to 2020. The quadratic regression model analysis in Figure 2a shows slightly better performance than its linear counterpart in capturing the variance between VM and intense TCGF over the SE-WNP (adjusted $R^2 = 0.84$ vs. 0.78; F-test for nonlinearity: $p = 0.038$). Phase-dependent analysis revealed two distinct regimes: Positive VM phase: TCGF shows a robust positive correlation with VM intensity ($r = 0.89$, $p = 0.02$), with about 63% of interannual variability explained by VM variability ($n = 35$ years). Negative VM phase: There is no statistically significant relationship ($r = 0.26$, $p = 0.12$; $n = 38$ years), suggesting that background dynamic controls outweigh VM influences under negative phase conditions (Figure 2a). We also tried classification criteria such as 0.75σ and 1σ , and the results show that the relationship between VM and intense TCGF is not sensitive to the choice of classification criteria. As illustrated in Figure 2b, the presence of VM with active-phase TCs was observed to exhibit threefold frequency dominance over inactive phases (72%:28%), which was further compounded by the emergence probabilities of intense TCs exceeding 4:1 (81%:19%).

To summarize, all these results show not only a strong correlation between the FMA VM and the SE-WNP TCGF but also that this relationship exhibits an asymmetric response of intense TCs to the VM. During positive VM years, more intense TCs form over the SE-WNP, typically coinciding with an increase in TCs across the whole WNP basin, while negative VM years have only a minor impact on the intense TCGF over the same subbasin. Overall, the VM would modify the genesis frequency of intense TCs by influencing the overall TCGFs over SE-WNP.

4. Asymmetric Response of Environmental Conditions to the VM

To investigate the underlying mechanisms behind the asymmetric response of intense TC over the SE-WNP to VM, we further analyze the lagged regression diagnostics between the FMA VMI and subsequent North Pacific

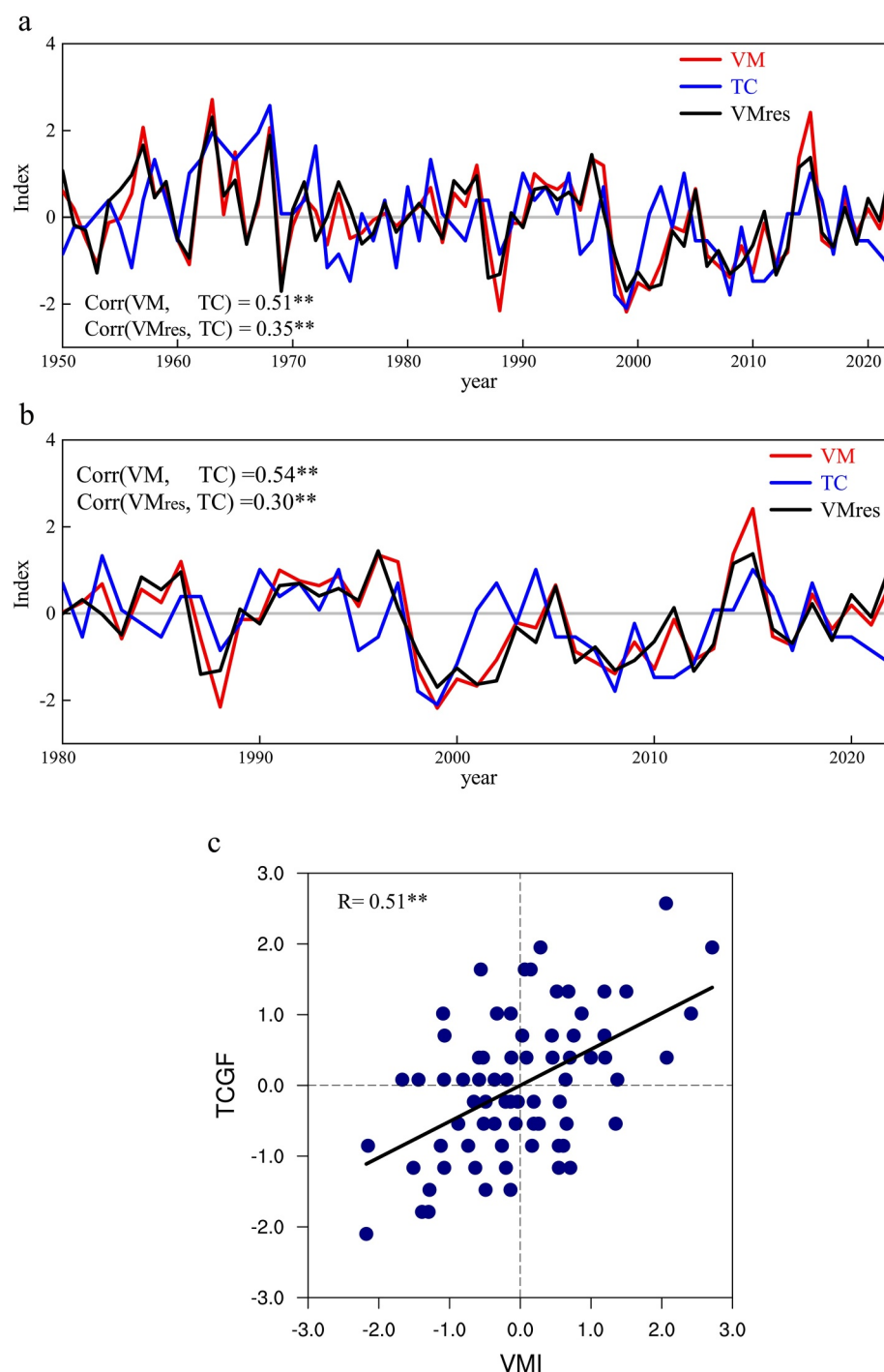


Figure 1. (a) Evolution over time of the annual variations of the JJASO southeastern western North Pacific (SE-WNP) tropical cyclone genesis frequency (TCGF) (blue line), the FMA Victoria mode (VM) indices (red line) and the VM index removal of contemporaneous Nino 3.4 indices (VM_{res}; black line) during 1950–2022. (b) Same as (a), but for 1980–2022. (c) Scatterplot of the FMA VM index with the JJASO SE-WNP TCGF. The correlation coefficient and significance level are on the top left of the panel.

SST)/surface wind anomalies (Figure 3). In positive VM phases, spring exhibits a meridional three-pole SST anomaly structure across the basin: Warm anomalies span from coastal North America to the central equatorial Pacific, flanked by subtropical anomalies sustained through TC season via subtropical wind-evaporation-SST coupling (WES mechanism; Xie & Philander, 1994). These maintained subtropical thermal anomalies

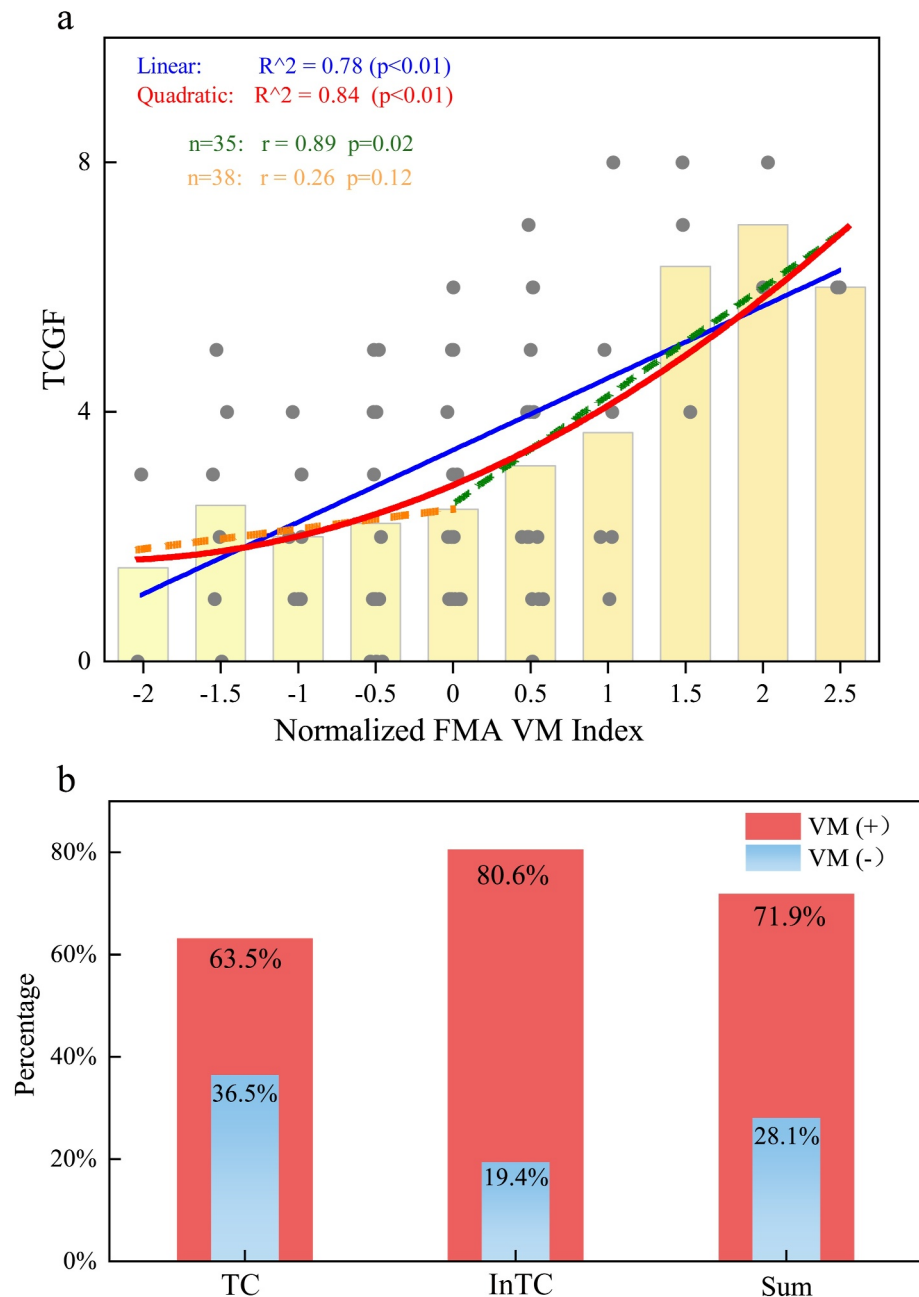


Figure 2. (a) Relationship between the intense tropical cyclone genesis frequency over southeastern western North Pacific (SE-WNP) during JJASO and the normalized FMA Victoria mode (VM) index from 1950 to 2022. Vertical gold bars represent kernel density estimates of intense tropical cyclone (TC) frequency distribution across the VM index. The gray dots indicate the frequency of intense TCs at a particular VM index. Solid blue and red curves depict optimal linear and quadratic regression models, respectively, with associated determination coefficients (R^2) and statistical significance annotated in panel insets. Phase-segregated analyses: emerald and amber dashed lines indicate distinct linear regressions for $\pm 0.5\sigma$ VM thresholds (positive phase: $n = 35$; negative phase: $n = 38$); corresponding Pearson correlations (r) with p -values displayed in the upper-left quadrant. (b) Positive/negative VM phase diagnostics (red/blue histograms) quantify SE-WNP TC intensity partitioning, with wind speed categorical thresholds—intense TC (InTC; ≥ 51.0 m/s), TC (32.7–50.9 m/s)—annotating proportional stratifications.

subsequently drive atmospheric adjustments that generate tropical SST anomalies through the seasonal footprinting mechanism (SFM; Vimont et al., 2003). In contrast, the negative SST anomalies in the central North Pacific gradually weakened. Meanwhile, a significant latitudinal SST anomaly gradient formed between the

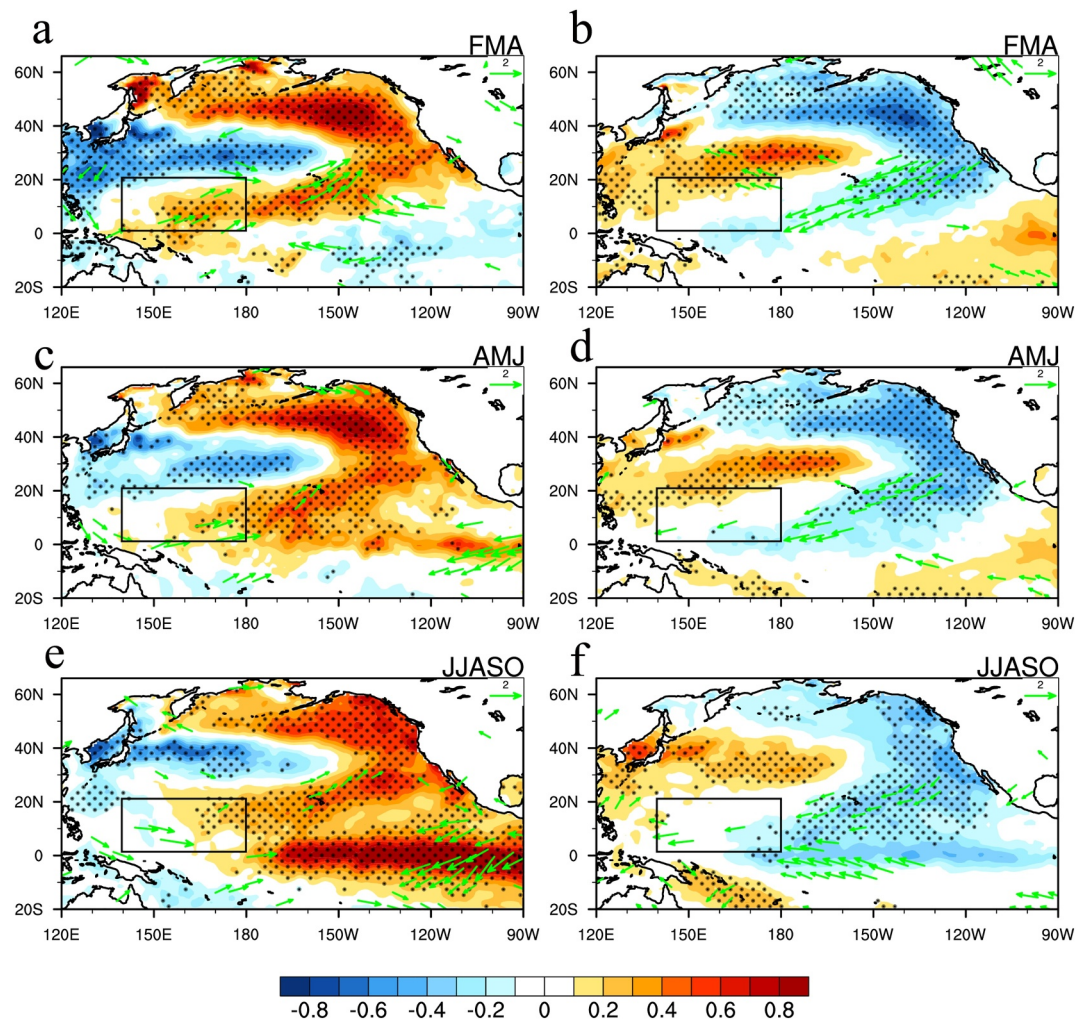


Figure 3. The regression maps show the relationship between the FMA Victoria mode (VM) index and the 3-month averaged sea surface temperature (shaded) and 850-hPa wind (vectors) anomalies for FMA, AMJ, and JJASO during positive VM years (left) and negative VM years (right). Statistically robust signals ($\alpha = 0.05$ via two-tailed Student's t -test) are encoded as black stippling for SSTACs. Surface winds retain vector visibility only where their zonal/meridional components reject stationarity assumptions ($p < 0.05$). Boxes in (a–f) indicate the southeastern western North Pacific (0° – 20° N, 140° – 180° E).

warming in the central-eastern equatorial Pacific and the cooling in the northwestern Pacific, altering the original latitudinal thermal difference between the regions and stimulating a large-scale westerly anomaly in the western equatorial Pacific. These westerly surface wind anomalies may provide favorable conditions for TC generation and development by increasing low-level convergence, vorticity, and weakening VWS. This will be discussed in more details later.

Comparison of the evolutions of SSTs and wind fields shows a significant difference during negative and positive VM years. During FMA, the subtropical northeastern Pacific exhibits concentrated negative SSTAs. These SSTAs extend and persist into the equatorial CP during JJASO, consistent with the evolution of the wind field. Concurrently, elevated positive SSTAs manifest as a longitudinally extensive band across the WNP's midlatitude zone. The SSTA change during negative VM years exhibits a narrow, statistically insignificant range. In contrast, positive VM years are characterized by a wide, statistically significant range of SSTA change (Figure 3). These findings reveal disparate reactions in Pacific SSTAs and near-surface wind patterns to the VM. In general, positive VM years are higher and associated with higher SFM than negative ones. However, the SE-WNP (intense) TCGF does not decrease significantly under negative VM years, suggesting that the influence of TCGF is not only related to the SST and wind field but also to other environmental fields. Although the area of

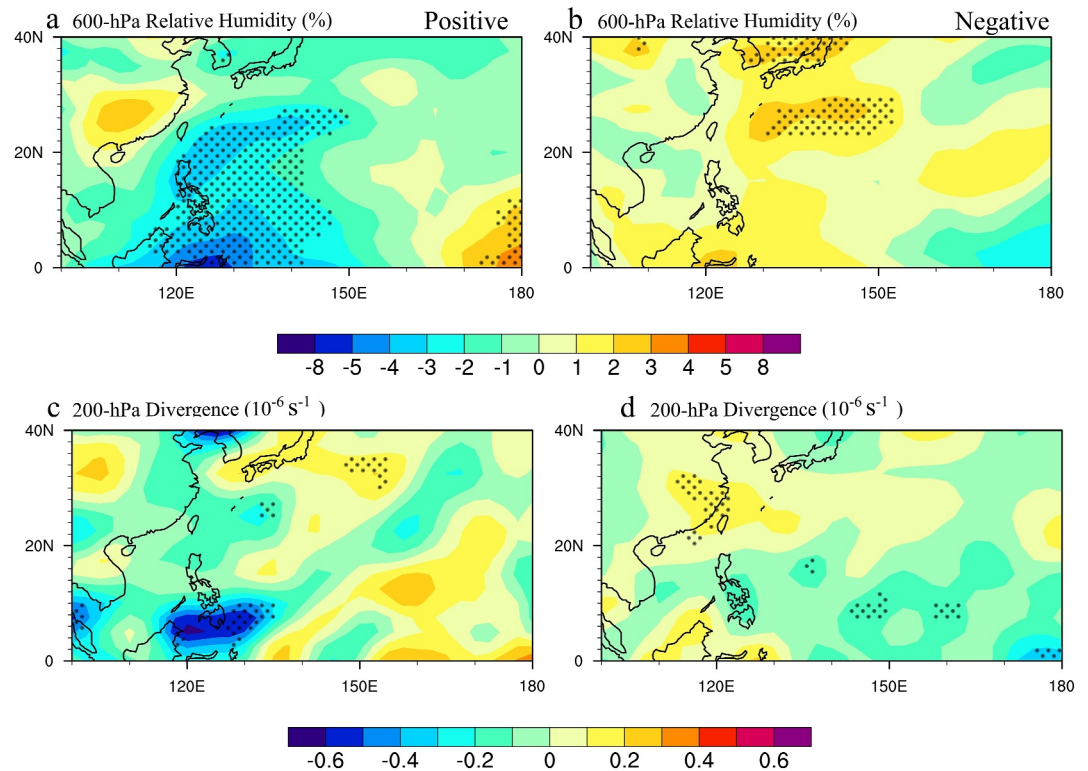


Figure 4. Anomalies of (a) 600-hPa relative humidity and (c) 200-hPa divergence during positive Victoria mode (VM) events. Panels (b) and (d) are same as (a) and (c), but for anomalies during negative VM events. Statistical significance ($p < 0.05$) is indicated by stipples.

significantly warm JJASO mean SST anomaly over the SE-WNP in positive VM is larger than the area of significantly cool JJASO mean SST anomaly over the SE-WNP in negative VM (with an area ratio of 1.8:1), the amplitude is relatively symmetric, exhibiting average SST anomalies of $+0.32^{\circ}\text{C}$ and -0.28°C in the respective phases.

Previous studies have suggested that extratropical influences on WNP TC behavior are principally driven by alterations in broader atmospheric parameters (Liu et al., 2019; Pu et al., 2019; Song et al., 2023; Wang & Wu, 2024). Therefore, we compare environmental variable deviations between opposing VM phases against the 1950–2022 chronological baseline (Figures 4 and 5). During positive VM events, while pronounced midtropospheric moisture deficits dominate near the International Date Line, limited hydrological variability occurs along the eastern periphery of 150°E , whereas during negative VM events, basin-wide coherence in relative humidity anomalies is observed. 200-hPa divergence shows no significant changes over most of the WNP during positive VM events, while the negative VM shows an overall weakening over SE-WNP (Figure 4). This evidence indicates that thermodynamic elements—including upper-level divergence and midtropospheric moisture content—exert limited regulatory influence on SE-WNP TC generation and development across VM events.

By comparison, kinematic parameters have a greater modulatory influence than thermodynamic controls. Many studies suggested that these changes in the dynamic conditions will lead to an increase in both the genesis frequency and intensity of TCs (Gao et al., 2021; Schade, 2000; Shan et al., 2023). Within the SE-WNP, the midlevel rotation dynamics show pronounced 850-hPa relative vorticity enhancements across the 10° – 30°N tropical-subtropical transition zone (Figure 5a). Furthermore, a significant decrease in 850–200-hPa VWS is observed in most of the SE-WNP region (Figure 5c). These provide the basic conditions necessary for the TC formation and a stable environment for their development. Compared to the anomalies of thermodynamic factors, significant anomalies in relative vorticity and VWS correspond to a much larger area (Figure 4). This suggests that 850-hPa relative vorticity and 850–200-hPa VWS are likely the primary factors affecting the genesis frequency and intensity of TCs during positive VM years.

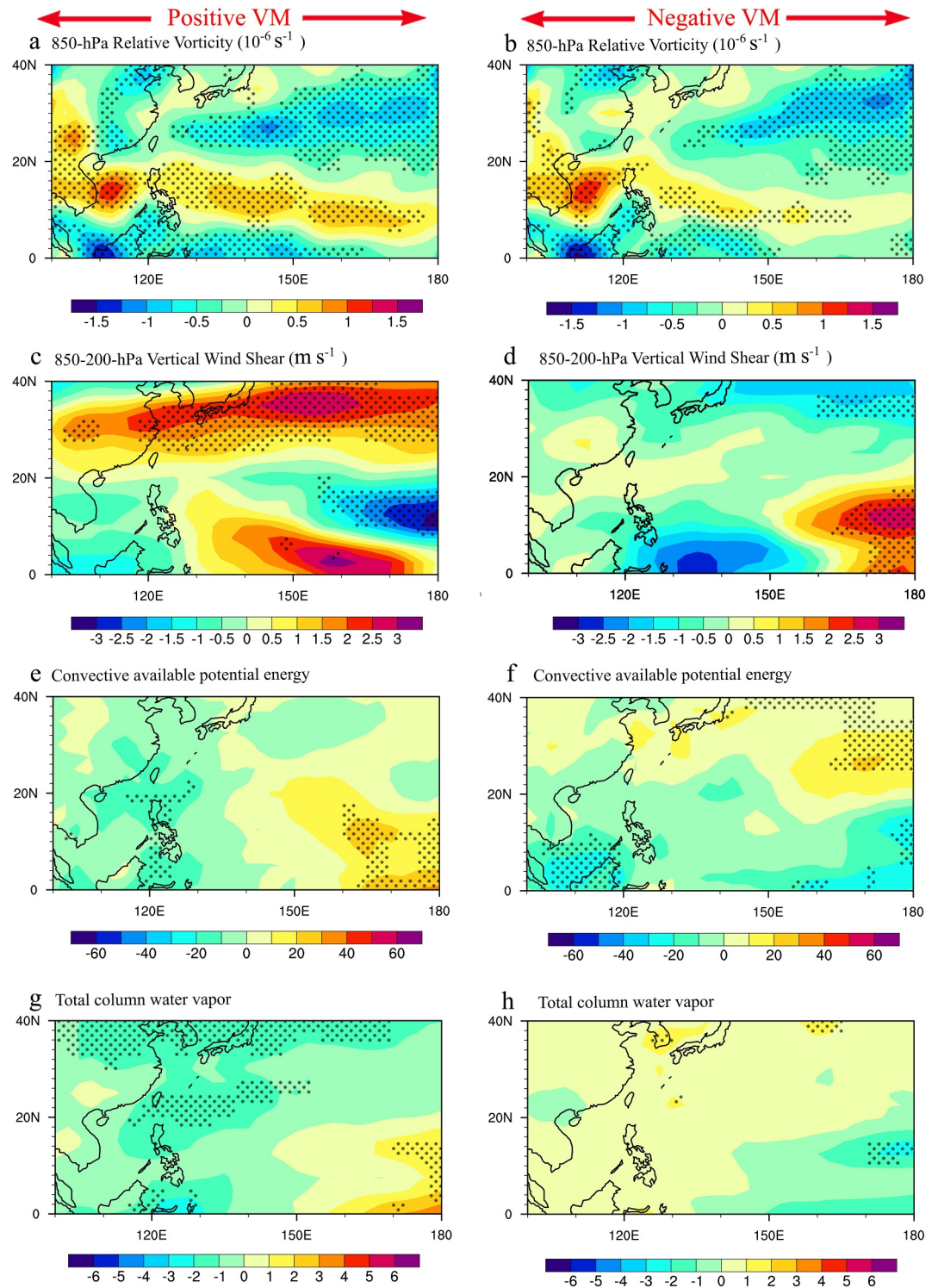


Figure 5. Anomalies of (a) 850-hPa relative vorticity, (c) 850–200-hPa vertical wind shear, (e) convective available potential energy, and (f) total column water vapor during positive Victoria mode (VM) years. Panels (b), (d), (f), and (h) are same as (a), (c), (e), and (g) but for anomalies during negative VM years. Statistical significance ($p < 0.05$) is indicated by stipples.

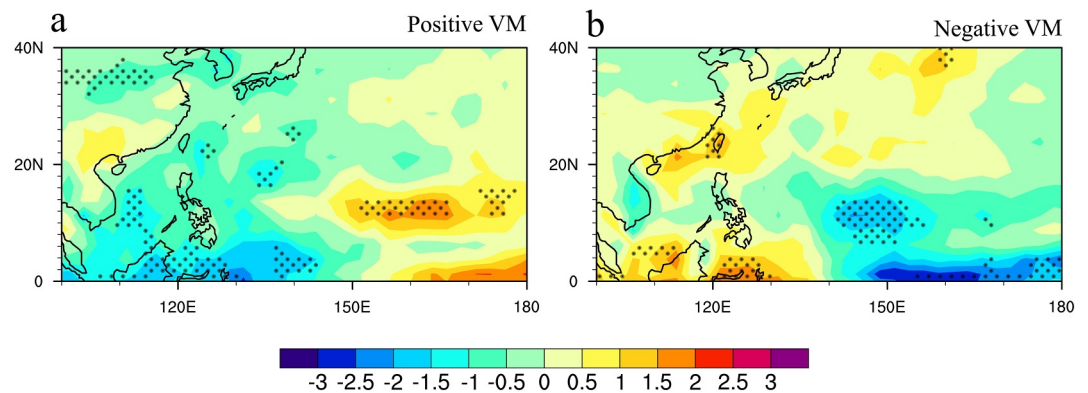


Figure 6. Anomalies of (a) precipitation (shading; mm/month) during positive Victoria mode (VM) years. Panel (b) is the same as (a), but for anomalies during negative VM years. Statistical significance ($p < 0.05$) is indicated by stipples.

Meanwhile, the CAPE is strengthened during positive VM events (Figure 5e), which encourage TC development. In addition, the SSTs in the SE-WNP exhibit an increase during positive VM events (Figure 3). Thermodynamic scaling principles (Clausius-Clapeyron, $\sim 7\%^\circ\text{C}^{-1}$) dictate amplified moisture advection under warming conditions, catalyzing deep convective destabilization (Figure 5c) and more positive precipitation anomalies (Figure 6a). As a result, a significant increase in TCWV exhibits over the WNP basin during positive VM events (Figure 5g). The combination of high CAPE and high TCWV favors the formation and development of strong convection. This strong convection heats the upper troposphere by releasing latent heat, which lowers the atmospheric pressure and creates low-pressure systems. These conditions persist and are accompanied by sufficiently high SST for the low-pressure system to be more favorable for development into a TC. During the development of TC, higher values of CAPE and TCWV mean that there is more energy and water vapors to support stronger updrafts and more latent heat release, allowing the TC to intensify further. The promotional effect is much weaker in the region of low values. This asymmetry in thermodynamic energy budgets—substantial intensification versus marginal suppression—explains the nonlinear TCGF response.

The 850-hPa relative vorticity has a similar division pattern during both the positive/negative VM events, but the magnitude is much larger for the former than those for the latter (Figures 5a and 5b). Additionally, CAPE and TCWV exhibit significantly negative anomalies in most of the SE-WNP (Figures 5f and 5h), consistent with negative precipitation anomalies (Figure 6b). In particular, the 850–200-hPa VWS anomaly configurations between opposing VM phases demonstrate inverse symmetry ($r = -0.52$; $p < 0.01$; Figures 5c and 5d). These findings reveal the asymmetric response of low-level circulation anomalies during different VM phases, with larger magnitudes of circulation anomalies during positive VM events compared to negative VM events. In general, most environmental conditions during positive VM events are not only favorable for TCGF but also inherently conducive to TC development. In contrast, only vorticity anomalies are conducive to TC genesis and subsequent development during negative VM events (Figure 5b). Overall, observational analyses show that the VM controls the generation and development of TCs through its influence on the atmospheric circulation over SE-WNP.

A quantitative analysis of asymmetric environmental responses reveals that VM phase polarity governs tropical cyclogenesis sensitivity through threshold-dependent intensity thresholds and multiscale couplings. Across the SE-WNP, the regional-averaged amplitude ratios of absolute anomalies (positive to negative VM events) are 1.8 for 850-hPa relative vorticity, 1.5 for vertical wind shear, 2.3 for CAPE, 2.6 for TCWV, and 2.0 for precipitation, demonstrating systematically stronger environmental modulation during positive VM events (Figure 7).

Considering that total SST is a necessary condition for tropical deep convection, a critical SST threshold exists that depends on the region and season (Graham & Barnett, 1987). Therefore, we further analyze the potential influence of the total SST over SE-WNP in both positive and negative VM on the asymmetric response of atmospheric environmental fields. Firstly, total SST over the SE-WNP in both VM+ and VM- years consistently exceeds the 27.5°C threshold, critical for deep tropical convection (Graham & Barnett, 1987). Moreover, we calculated the total SSTs in the SE-WNP core region across all VM+ and VM- years (1950–2022). Results show that all of VM+ and VM- years have JJASO area-averaged total SSTs $>28.0^\circ\text{C}$ over SE-WNP, well above the

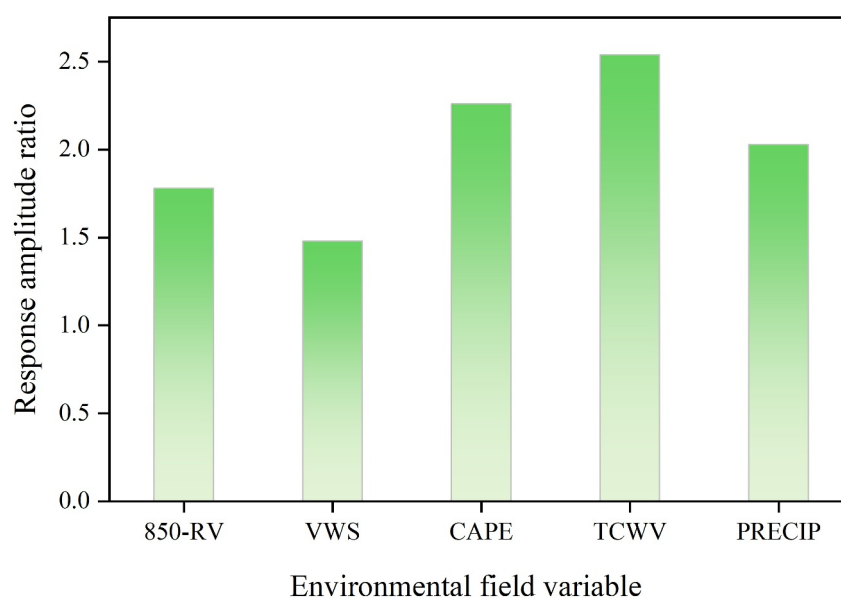


Figure 7. Response amplitude ratios of key environmental variables (positive to negative Victoria mode events) over the southeastern western North Pacific.

convection threshold. This indicates that the background SSTs in the SE-WNP during both VM phases are sufficient to sustain convection, and their minor differences cannot explain the observed asymmetry in environmental parameters (e.g., vorticity, vertical wind shear). The asymmetric response instead arises from how SST anomaly patterns modulate atmospheric dynamics: VM+ enhances WNP convection via amplified low-level westerlies and moisture convergence tied to its subtropical-extratropical dipole structure, while VM- weakens these processes due to suppressed air-sea coupling efficiency. Thus, while total SSTs precondition convective potential equally in both phases, the spatial structure of SST anomalies (not absolute SSTs) governs the asymmetry in environmental feedbacks.

Instead, the observed asymmetry in intense TCGF and environmental conditions arises from phase-specific nonlinear interactions between VM-related SST anomalies and atmospheric dynamics. During positive VM events, the persistence of subtropical SST anomalies—linked to VM—extends into the TC season WES feedbacks (Xie & Philander, 1994). These subtropical anomalies force tropical SST adjustments through the SFM, where warming in the central-eastern equatorial Pacific and cooling in the northwestern Pacific weaken the zonal SST gradient (Vimont et al., 2003). This gradient reduction drives westerly surface wind anomalies over the western equatorial Pacific, enhancing low-level convergence, increasing vorticity, and reducing vertical wind shear—collectively favoring TC genesis. In contrast, negative VM phases fail to sustain comparable dynamical coupling: central North Pacific cold anomalies decay seasonally, resulting in weaker background westerlies and suppressed energy conversion efficiency (Ding, Li, Tseng, & Ruan, 2015). Thus, while VM SST patterns are symmetric, their atmospheric teleconnections exhibit dramatic phase-dependent nonlinearity, driven by differences in feedback strength (e.g., WES efficiency) and background state modulation. This highlights the VM's capacity to amplify or dampen Pacific TC activity through asymmetric atmospheric pathways, despite its symmetric oceanic expression.

Next, we further examine the composite differences in environmental fields obtained from two CESM ensemble experiments. Over the SE-WNP, changes in precipitation show significantly positive anomalies and the westerly surface wind anomalies are exceptionally strong (Figure 8a). Analogous vorticity perturbations occur within the thermocline ridge corridor of the equatorial Pacific (Figure 8b), consistent with the observed results (Figure 5c). Favorable conditions for TC formation were created by the presence of anomalous westerly surface wind anomalies over the equatorial western Pacific. This is coupled with enhanced convective activity, establishing a mutually reinforcing vertical mass flux feedback loop, thereby promoting the development of updrafts and sustained convective processes (Choi et al., 2024). Empirical evidence for these dynamics is provided by the positive precipitation anomalies over the SE-WNP (Figure 8a), consistent with positive precipitation anomalies in

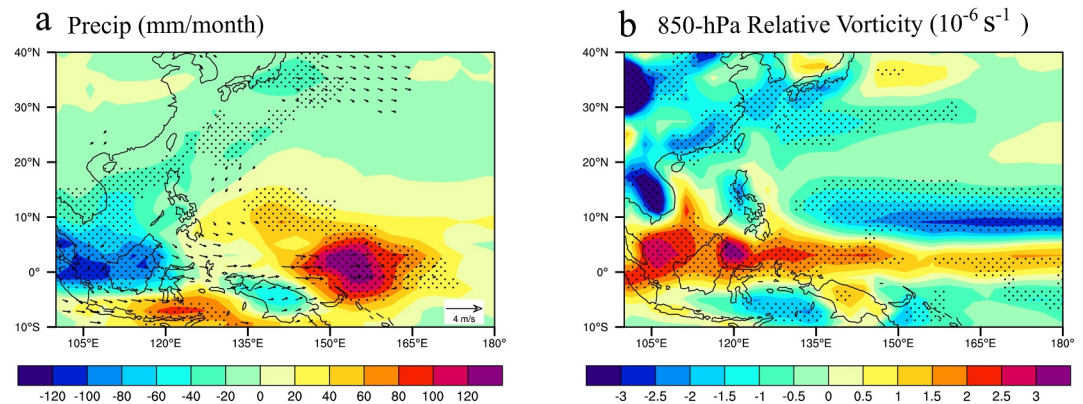


Figure 8. (a) Composite differences in 850-hPa wind and precipitation (shading; mm/month) between the positive and negative Victoria mode run from the CESM. Panel (b) same as (a), but for 850-hPa relative vorticity. Statistical significance ($p < 0.05$) is indicated by dashed symbols. Only surface wind vectors with statistical significance ($p < 0.05$) are shown.

observed results (Figure 6a). These results indicate that the environmental fields associated with positive VM events are indeed more conducive to TC generation and development than that of observed and simulated variable fields during negative VM events.

5. Summary and Discussion

This study highlights a significantly asymmetric response of intense TCGF over SE-WNP during JJASO to the different phases of the VM from 1950 to 2022. Curvilinear interdependencies between the VM and TCGF surpass the statistical validity of previously hypothesized linear couplings by Pu et al. (2019). As demonstrated by both observational analyses and numerical simulations, the asymmetric responses of intense TCGF to VM are explained by distinct alterations in environmental conditions under contrasting VM events over SE-WNP. On average, positive VM phases manifest expansive subtropical-tropical Pacific thermal dipoles: Warm anomalies spanning 20°N–10°S midbasin contrasting cold equator-east Pacific anomalies, coupled with zonal wind reversals modulating Hadley circulation structures. These synergistic thermodynamic-kinetics adjustments—including vorticity enrichment, convective energy accumulation, and vertical shear suppression—collectively prime the basin-scale cyclogenesis environment. Of the environmental factors under consideration, 850-hPa relative vorticity and VWS are likely to be of the greatest importance in terms of the genesis and development of TCs. In contrast, negative VM event perturbations have been observed to confine thermal anomalies to the subtropical Pacific region. This phenomenon involves the coupling of reversed zonal flow cells with the propagation of cold pools. Consequently, substantial fluctuations in large-scale circulations over the WNP are rarely observed as a result of negative VM, signifying that environmental anomalies manifest at reduced magnitudes and lack statistical significance over SE-WNP.

Although this study focuses on the VM-TC correlation in recent modern observations in the warmer climate (Ji et al., 2024), interdecadal variations in VM intensity linked to the PDO locus may further modulate TC activity. This will be explored in future work to use the reanalysis data set and CESM2 pacemaker simulations to clarify VM-PDO phase synchronization for climate warming modulation.

Conflict of Interest

The authors declare no conflicts of interest relevant to this study.

Data Availability Statement

We are grateful for access to the following freely available data: the HadISST data set obtained from the Met Office (<https://www.metoffice.gov.uk/hadobs/hadsst3/data/download.html>); the ERA5 reanalysis data are available at cds.climate.copernicus.eu and <https://doi.org/10.24381/cds.f17050d7>; the NCEP/NCAR Reanalysis 1 data were obtained from their website (<https://www.esrl.noaa.gov/psd/data/gridded/data.ncep.reanalysis.html>);

and the tropical cyclone best-track data from the International Best Track Archive for Climate Stewardship (IBTrACS) were obtained from their website (<https://www.ncei.noaa.gov/data/international-best-track-archive-for-climate-stewardship-ibtracs/v04r01/access/netcdf/>).

Acknowledgments

This research was jointly supported by the National Natural Science Foundation of China (42225501, 42105059) and China's National Key Research and Development Projects (2020YFA0608400). In addition, Wentao wants to thank Mao Yilu for her assistance, in particular. CORE is a joint research center for ocean research between Laoshan Laboratory and HKUST.

References

- Chen, S., Chen, W., Yu, B., Wu, L., Chen, L., Li, Z., et al. (2023). Impact of the winter Arctic sea ice anomaly on the following summer tropical cyclone genesis frequency over the western North Pacific. *Climate Dynamics*, 61(7), 3971–3988. <https://doi.org/10.1007/s00382-023-06789-5>
- Choi, H.-Y., Park, M.-S., Kim, H.-S., & Lee, S. (2024). Marine heatwave events strengthen the intensity of tropical cyclones. *Communications Earth & Environment*, 5(1), 69. <https://doi.org/10.1038/s43247-024-01239-4>
- Chu, P.-S., Zhao, X., Ho, C.-H., Kim, H.-S., Lu, M.-M., & Kim, J.-H. (2010). Bayesian forecasting of seasonal typhoon activity: A track-pattern-oriented categorization approach. *Journal of Climate*, 23(24), 6654–6668. <https://doi.org/10.1175/2010JCLI3710.1>
- Di Lorenzo, E., & Mantua, N. (2016). Multi-year persistence of the 2014/15 North Pacific marine heatwave. *Nature Climate Change*, 6(11), 1042–1047. <https://doi.org/10.1038/nclimate3082>
- Ding, R., Li, J., Tseng, Y.-h., & Ruan, C. (2015). Influence of the North Pacific Victoria mode on the Pacific ITCZ summer precipitation. *Journal of Geophysical Research: Atmospheres*, 120(3), 964–979. <https://doi.org/10.1002/2014JD022364>
- Ding, R., Li, J., Tseng, Y.-h., Sun, C., & Guo, Y. (2015). The Victoria mode in the North Pacific linking extratropical sea level pressure variations to ENSO. *Journal of Geophysical Research: Atmospheres*, 120(1), 27–45. <https://doi.org/10.1002/2014JD022221>
- Ding, R., Nnamchi, H. C., Yu, J. Y., Li, T., Sun, C., Li, J., et al. (2023). North Atlantic oscillation controls multidecadal changes in the North tropical Atlantic–pacific connection. *Nature Communications*, 14(1), 862. <https://doi.org/10.1038/s41467-023-36564-3>
- Ding, R., Tseng, Y., Di Lorenzo, E., Shi, L., Li, J., Yu, J. Y., et al. (2022). Multi-year El Niño events tied to the North Pacific oscillation. *Nature Communications*, 13(1), 3871. <https://doi.org/10.1038/s41467-022-31516-9>
- Gao, S., Mao, J., Zhang, W., Zhang, F., & Shen, X. (2021). Atmospheric moisture shapes increasing tropical cyclone precipitation in southern China over the past four decades. *Environmental Research Letters*, 16(3), 034004. <https://doi.org/10.1088/1748-9326/abd78a>
- Graham, N. E., & Barnett, T. P. (1987). Sea surface temperature, surface wind divergence, and convection over tropical oceans. *Science*, 238(4827), 657–659. <https://doi.org/10.1126/science.238.4827.657>
- Guo, Y. P., & Tan, Z. M. (2018). Westward migration of tropical cyclone rapid-intensification over the Northwestern Pacific during short duration El Niño. *Nature Communications*, 9(1), 1507. <https://doi.org/10.1038/s41467-018-03945-y>
- Huang, M., Wang, Q., Liu, M., Lin, N., Wang, Y., Jing, R., et al. (2022). Increasing typhoon impact and economic losses due to anthropogenic warming in Southeast China. *Scientific Reports*, 12(1), 14048. <https://doi.org/10.1038/s41598-022-17323-8>
- Huang, R., Chen, S., Chen, W., Wu, R., Wang, Z., Hu, P., et al. (2024). Impact of the winter regional hadley circulation over Western Pacific on the frequency of following summer tropical cyclone landfalling in China. *Journal of Climate*, 37(13), 3521–3541. <https://doi.org/10.1175/JCLI-D-23-0610.1>
- Hurrell, J. W., Holland, M. M., Gent, P. R., Ghan, S., Kay, J. E., Kushner, P. J., et al. (2013). The community Earth system model: A framework for collaborative research. *Bulletin of the American Meteorological Society*, 94(9), 1339–1360. <https://doi.org/10.1175/BAMS-D-12-00121.1>
- Ji, K., Yu, J.-Y., Li, J., Hu, Z.-Z., Tseng, Y.-H., Shi, J., et al. (2024). Enhanced North Pacific Victoria mode in a warming climate. *npj Climate and Atmospheric Science*, 7(1), 49. <https://doi.org/10.1038/s41612-024-00599-0>
- Kalnay, E., Kanamitsu, M., Kistler, R., Collins, W., Deaven, D., Gandin, L., et al. (1996). The NCEP/NCAR 40-Year reanalysis project. *Bulletin of the American Meteorological Society*, 77(3), 437–472. [https://doi.org/10.1175/1520-0477\(1996\)077<0437:TNYRP>2.0.CO;2](https://doi.org/10.1175/1520-0477(1996)077<0437:TNYRP>2.0.CO;2)
- Kim, H.-K., Seo, K.-H., Yeh, S.-W., Kang, N.-Y., & Moon, B.-K. (2020). Asymmetric impact of central Pacific ENSO on the reduction of tropical cyclone genesis frequency over the western North Pacific since the late 1990s. *Climate Dynamics*, 54(1), 661–673. <https://doi.org/10.1007/s00382-019-05020-8>
- Knapp, K. R., Kruk, M. C., Levinson, D. H., Diamond, H. J., & Neumann, C. J. (2010). The international best track archive for climate stewardship (IBTrACS): Unifying tropical cyclone data. *Bulletin of the American Meteorological Society*, 91(3), 363–376. <https://doi.org/10.1175/2009BAMS2755.1>
- Kunze, S. (2021). Unraveling the effects of tropical cyclones on economic sectors worldwide: Direct and indirect impacts. *Environmental and Resource Economics*, 78(4), 545–569. <https://doi.org/10.1007/s10640-021-00541-5>
- Li, C., Wang, C., & Zhao, T. (2018). Influence of two types of ENSO events on tropical cyclones in the western North Pacific during the subsequent year: Asymmetric response. *Climate Dynamics*, 51(7), 2637–2655. <https://doi.org/10.1007/s00382-017-4033-y>
- Li, J., Sun, C., & Jin, F.-F. (2013). NAO implicated as a predictor of Northern hemisphere mean temperature multidecadal variability. *Geophysical Research Letters*, 40(20), 5497–5502. <https://doi.org/10.1002/2013GL057877>
- Li, W., Li, L., & Deng, Y. (2015). Impact of the interdecadal Pacific oscillation on tropical cyclone activity in the north Atlantic and eastern north Pacific. *Scientific Reports*, 5(1), 12358. <https://doi.org/10.1038/srep12358>
- Liu, C., Zhang, W., Stuecker, M. F., & Jin, F.-F. (2019). Pacific meridional mode-western North Pacific tropical cyclone linkage explained by tropical Pacific quasi-decadal variability. *Geophysical Research Letters*, 46(22), 13346–13354. <https://doi.org/10.1029/2019GL085340>
- Lu, X., Yu, H., Ying, M., Zhao, B., Zhang, S., Lin, L., et al. (2021). Western North Pacific tropical cyclone database created by the China meteorological administration. *Advances in Atmospheric Sciences*, 38(4), 690–699. <https://doi.org/10.1007/s00376-020-0211-7>
- Murnane, R. J., & Elsner, J. B. (2012). Maximum wind speeds and US hurricane losses. *Geophysical Research Letters*, 39(16), L16707. <https://doi.org/10.1029/2012GL052740>
- Newman, M., Alexander, M. A., Ault, T. R., Cobb, K. M., Deser, C., Di Lorenzo, E., et al. (2016). The Pacific decadal oscillation, revisited. *Journal of Climate*, 29(12), 4399–4427. <https://doi.org/10.1175/JCLI-D-15-0508.1>
- Pu, X., Chen, Q., Zhong, Q., Ding, R., & Liu, T. (2019). Influence of the North Pacific Victoria mode on western North Pacific tropical cyclone genesis. *Climate Dynamics*, 52(1), 245–256. <https://doi.org/10.1007/s00382-018-4129-z>
- Pyper, B. J., & Peterman, R. M. (1998). Comparison of methods to account for autocorrelation in correlation analyses of fish data. *Canadian Journal of Fisheries and Aquatic Sciences*, 55(9), 2127–2140. <https://doi.org/10.1139/f98-104>
- Salinger, M. J., Renwick, J. A., & Mullan, A. B. (2001). Interdecadal Pacific oscillation and south Pacific climate. *International Journal of Climatology*, 21(14), 1705–1721. <https://doi.org/10.1002/joc.691>
- Schade, L. R. (2000). Tropical cyclone intensity and sea surface temperature. *Journal of the Atmospheric Sciences*, 57(18), 3122–3130. [https://doi.org/10.1175/1520-0469\(2000\)057<3122:TCLASS>2.0.CO;2](https://doi.org/10.1175/1520-0469(2000)057<3122:TCLASS>2.0.CO;2)

- Scoccimarro, E., Villarini, G., Gualdi, S., & Navarra, A. (2021). The Pacific decadal oscillation modulates tropical cyclone days on the interannual timescale in the North Pacific Ocean. *Journal of Geophysical Research: Atmospheres*, 126(15), e2021JD034988. <https://doi.org/10.1029/2021jd034988>
- Shan, K., Lin, Y., Chu, P.-S., Yu, X., & Song, F. (2023). Seasonal advance of intense tropical cyclones in a warming climate. *Nature*, 623(7985), 83–89. <https://doi.org/10.1038/s41586-023-06544-0>
- Song, J., Klotzbach, P. J., Wang, Y.-F., & Duan, Y. (2023). Asymmetric influence of the Pacific meridional mode on tropical cyclone formation over the western North Pacific. *International Journal of Climatology*, 43(14), 6578–6589. <https://doi.org/10.1002/joc.8220>
- Vimont, D. J., Wallace, J. M., & Battisti, D. S. (2003). The seasonal footprinting mechanism in the Pacific: Implications for ENSO. *Journal of Climate*, 16(16), 2668–2675. [https://doi.org/10.1175/1520-0442\(2003\)016<2668:TSFMIT>2.0.CO;2](https://doi.org/10.1175/1520-0442(2003)016<2668:TSFMIT>2.0.CO;2)
- Wang, J., & Wu, Z. (2023). Distinctive features of Monsoon-TC joint rainfall over Western North Pacific and its relationship with the maritime continent thermal condition. *Atmosphere-Ocean*, 61(5), 318–334. <https://doi.org/10.1080/07055900.2023.2221217>
- Wang, J., & Wu, Z. (2024). Three types of East Asian summer rainfall associated with monsoon circulation and tropical cyclone activities: Unique features and major influential factors. *Climate Dynamics*, 62(5), 4099–4116. <https://doi.org/10.1007/s00382-024-07120-6>
- Wang, Q., Li, J., Jin, F. F., Chan, J. C. L., Wang, C., Ding, R., et al. (2019). Tropical cyclones act to intensify El Niño. *Nature Communications*, 10(1), 3793. <https://doi.org/10.1038/s41467-019-11720-w>
- Wang, Q., Li, J., Li, Y., Xue, J., Zhao, S., Xu, Y., et al. (2019). Modulation of tropical cyclone tracks over the western North Pacific by intra-seasonal indo-western Pacific convection oscillation during the boreal extended summer. *Climate Dynamics*, 52(1), 913–927. <https://doi.org/10.1007/s00382-018-4264-6>
- Wu, Z., & Lin, H. (2012). Interdecadal variability of the ENSO–North Atlantic Oscillation connection in boreal summer. *Quarterly Journal of the Royal Meteorological Society*, 138(667), 1668–1675. <https://doi.org/10.1002/qj.1889>
- Xie, S.-P., & Philander, S. G. H. (1994). A coupled ocean-atmosphere model of relevance to the ITCZ in the eastern Pacific. *Tellus A: Dynamic Meteorology and Oceanography*, 46(4), 340. <https://doi.org/10.3402/tellusa.v46i4.15484>
- Ying, M., Zhang, W., Yu, H., Lu, X., Feng, J., Fan, Y., et al. (2014). An overview of the China meteorological administration tropical cyclone database. *Journal of Atmospheric and Oceanic Technology*, 31(2), 287–301. <https://doi.org/10.1175/JTECH-D-12-00119.1>
- Zhan, R., Wang, Y., & Ding, Y. (2022). Impact of the western Pacific tropical easterly jet on tropical cyclone genesis frequency over the western North Pacific. *Advances in Atmospheric Sciences*, 39(2), 235–248. <https://doi.org/10.1007/s00376-021-1103-1>